Available online at www.sciencedirect.com
ScienceDirect
Applied Surface Science 253 (2006) 2154–2157
applied surface science
www.elsevier.com/locate/apsusc

Morphology and structure of gold–lithium niobate thin film: A laboratory source X-ray scattering study

S. Hazra

Surface Physics Division, Saha Institute of Nuclear Physics, 1/AF Bidhannagar, Kolkata 700 064, India

Received 3 March 2006; received in revised form 5 April 2006; accepted 6 April 2006
Available online 15 May 2006

Abstract

Laboratory source X-ray scattering set-up has been used to determine the complete morphology and structure of an optically important composite thin film. Analysis of grazing incidence small angle X-ray scattering, X-ray reflectivity and powder diffraction data of Au/$LiNbO_3$ thin film prepared by sequential deposition of gold and lithium niobate on float glass substrate suggest that the Au-nanocrystallites are dispersed in amorphous medium, which although have average separation but do not have any long range periodicity other than growth or z-direction. The morphology of the nanocomposite thin film determined through X-ray scattering measurements agrees well with the measured optical absorption.

PACS: 68.55.−a; 61.10.−I; 61.46.+w; 78.67.Bf

Keywords: Thin film structure and morphology; X-ray diffraction and scattering; Clusters; Nanoparticles; and nanocrystalline materials; Optical properties of nanocrystals and nanoparticles

1. Introduction

X-ray scattering is an important technique for determining the structure and morphology of materials in a nondestructive way [1,2]. Surface sensitive X-ray scattering is particularly important for thin films and multilayer [2–7]. Specular reflectivity measurements provide us information regarding the electron density profile (EDP) of the thin films along the growth (z) direction and diffuse scattering measurements provide us large in-plane correlated features. Both specular reflectivity and diffuse scattering have been extensively used for last few years mainly for stratified systems. However, for composite thin films and multilayer, where clusters of nanometer size are dispersed in a matrix, known as nanocomposite, it is essential to know the size and shape of the clusters and their distribution or arrangement in the matrix; as the properties [8–13] strongly related to its morphology. Morphological determination of such composite films has been recently started through newly developed grazing incidence small-angle X-ray scattering (GISAXS) technique using synchrotron source and two-dimensional (2D) detector [14–18]. However, very few attempted have been made so far for the GISAXS measurement using laboratory source [19] even for composite containing clusters of high scattering cross-section and in large amount. Ceramic thin films containing Au clusters are one such group of composites, which shows interesting optical properties and needs detail structural and morphological understanding.

In this letter, X-ray reflectivity, GISAXS and powder diffraction measurements using laboratory source X-ray scattering set-up have been combined to bring out the complete structure and morphology of a composite thin film, such as Au–$LiNbO_3$ multilayers prepared by sequential sputtering of Au and $LiNbO_3$ targets on float glass substrate. Optical property was then compared with such morphology.

2. Experiment

X-ray scattering measurements were carried out using a versatile X-ray diffractometer (VXRD) set-up. VXRD consists of a diffractometer (D8 Discover, Bruker AXS) with Cu source (sealed tube) followed by Göbel mirror to select and enhance Cu Kα radiation ($\lambda_0 = 1.54$ Å). The diffractometer has 2-circle goniometer [$\theta(\omega) - 2\theta$] with 1/4-circle Eulerian cradle as sample stage. The latter has two-circlular (χ and ϕ) and three-

E-mail address: satyajit.hazra@saha.ac.in.

0169-4332/$ – see front matter
doi:10.1016/j.apsusc.2006.04.017

translational (X, Y and Z) motion. Scattered beam was detected using either NaI scintillation (point) or HI-STAR area (2D) detector. The specular and off-specular X-ray reflectivity and powder diffraction measurements of the film were performed using line source and point detector, while GISAXS measurements were performed for a fixed incidence angle, just above the critical angle of the film, using point source and 2D detector. Line source was made point or circular using collimator. All measurements were performed in reflection geometry. For the reflectivity measurements 0.2 mm slits were placed on both sides of the sample, which gives the width of the direct beam about 0.02° and that decides the resolutions. While for the powder diffraction measurement slit width has been increased, this gives the width of the direct beam about 0.04°. However, the resolution in this case is the convoluted effect of this width with the separation of peak at an angle due to Cu $K\alpha_1$ and Cu $K\alpha_2$ wavelengths of different intensities present in the source, which is about 0.1° for 2θ of 40°. For GISAXS measurement, the HI-STAR detector has been masked to get rid of direct, specularly reflected as well as beams of low q_y values. The optical absorption measurements of the films were carried out using UV–vis spectrophotometer (GBC Cintra).

3. Results and discussion

The specular and off-specular X-ray reflectivity data are shown in Fig. 1. The reflectivity profile shows the value of nearly one due to total external reflection, then rounding near average critical wave vector (q_c) due to the high absorption, followed by a sharp decrease due to the surface roughness, and broad humps due to bilayer separation (d_L). The broad humps are also visible in the off-specular profiles. Kiessig fringes, which are the measure of the total film thickness (t), is almost absent. This indicates that the top surface roughness of the film is very high. However, very weak signature of the Kiessig

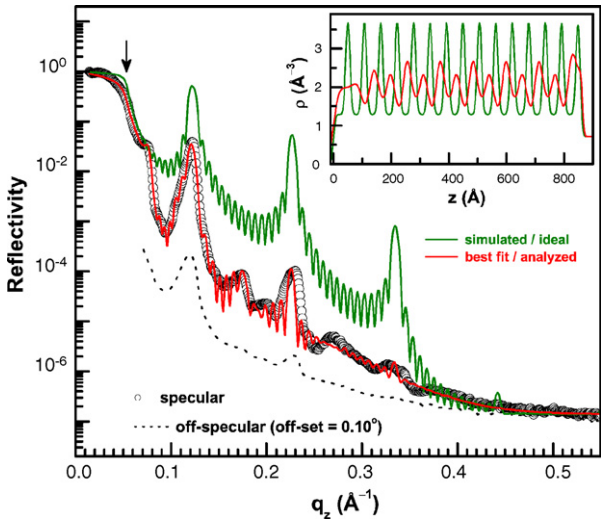

Fig. 1. Specular and off-specular reflectivity data of the Au/$LiNbO_3$ multilayer thin film. Arrow indicates the position of the average q_c of the film. Simulated and best-fit specular reflectivity profiles are for ideal and analyzed EDPs, respectively. Corresponding EDPs are shown in the inset.

fringes before first broad and sharp hump is observed, which has been utilized as the starting parameter of film thickness for the analysis carried out later.

The average critical wave vector ($q_{c,film} \sim 0.053$ Å^{-1}), obtained from the reflectivity curve is related to the average electron density (ρ) of the film and from that one can extract the volume fraction of Au in the film using following simple relation [15]:

$$f = \frac{\rho_{film} - \rho_{matrix}}{\rho_{Au} - \rho_{matrix}} = \frac{q_{c,film}^2 - q_{c,matrix}^2}{q_{c,Au}^2 - q_{c,matrix}^2}.$$

The q_c for Au is 0.079 Å^{-1} and that for $LiNbO_3$ is 0.043 Å^{-1}, which provide the volume fraction of Au in the film as 0.23. To obtain the EDP of the film, the reflectivity data has been analyzed using Parratt formalism [20] including roughness at each interface [21]. First we try to simulate the reflectivity profile considering perfect multilayer structure of the film, i.e. alternate layers of Au and $LiNbO_3$ with bulk electron density. The thickness was considered 14 and 43 Å, respectively, to satisfy the volume fraction (0.23) and also the bilayer separation (57 Å) arising from first sharp peak. Roughness at each interface was considered same and that of the substrate (6 Å). The simulated reflectivity profile thus obtained, however, deviates considerably. The major differences in the simulated reflectivity profile is that there is no signature of small broad peaks at around 0.17 and 0.27 Å^{-1}, also the intensity of the other broad peaks at around 0.12, 0.23 and 0.34 Å^{-1} is quite high compared to that of the experimental one.

To obtain the small broad peaks it is necessary to consider additional periodicity between two bilayers and to reduce the intensity of the others peaks it is necessary to reduce the contrast between Au and $LiNbO_3$ layers. Considering such ideology, we have clubbed 15 × 2 layers in three categories: First 2 layers just after substrate, then repetition of four layers by six times and on the top four layers. We then allow the thickness, electron density and roughness of 10 (2 + 4 + 4) layers as parameters and the best-fit curve thus obtained are shown in Fig. 1 along with the analyzed EDP in the inset. The agreement between the analyzed curve and the experimental data is fairly good in terms of major features. Analyzed EDP suggests a strong deviation form ideal multilayer structure, although still there. The high electron density positions in the EDP are due to the Au-layers. However, the low value compared to the density of bulk Au clearly indicates that the Au-layers are discontinues in x–y plane. If we try to overcome the discrepancies at large q_z values, we have to increase the number of free parameters, which we have avoided. Nonetheless, this essentially means there will be further deviation in the multilayer structure in terms of quantity, although qualitatively it may be the same.

Reciprocal space map of the film obtained from GISAXS measurement is shown in Fig. 2(a). The annular ring, which is related to the interparticles separation, is clearly evident in the figure. This also suggests that the multilayer structure is formed by clusters having definite size, shape and separation. For the

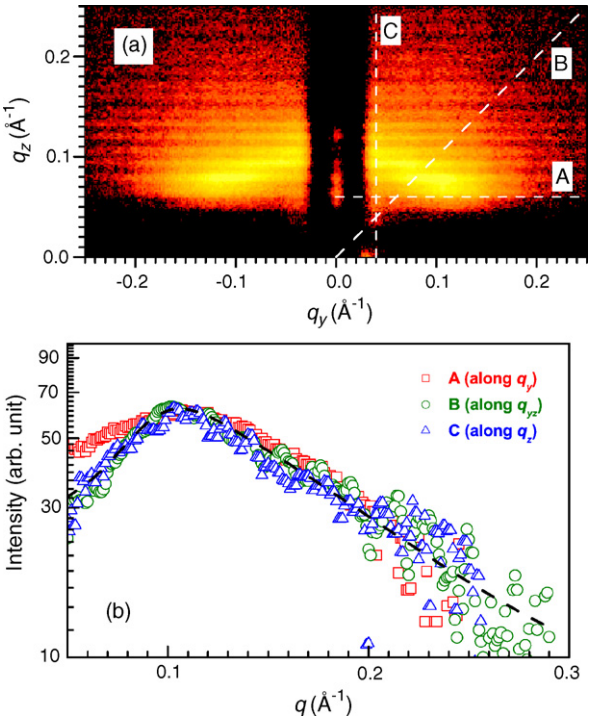

Fig. 2. (a) GISAXS image of the Au/$LiNbO_3$ multilayer thin film collected at fixed incidence angle. (b) Line profiles drawn through GISAXS image in different directions along with calculated one.

quantitative analysis, line profiles drawn through the GISAXS image in different directions are used. It was shown that if we consider spherical clusters of radius R are distributed in the matrix according to the cumulative disorder having average separation d, then the diffuse part can be considered arising from the clusters as [22–24]:

$$I_{\text{cluster}} \propto \frac{(\sin qR - qR\cos qR)^2}{(qR)^6} \frac{1 - e^{-2q^2\sigma_d^2}}{1 - 2\cos(qd)e^{-q^2\sigma_d^2} + e^{-2q^2\sigma_d^2}},$$

where σ_d is the variance of d. Above expression has been used to get the value of R and d from the GISAXS line profiles. Calculated line profile along with the experimental line profiles are shown in Fig. 2(b). The average particle size ($2R$) and separation (d) are found to be $\sim 32 \pm 4$ and 56 ± 16 Å, respectively, which agrees well with the analyzed EDP (inset of Fig. 1). The high value ($\sim$16 Å) of σ_d suggests that there is no long-range periodicity between clusters unlike z-direction.

The powder diffraction pattern of the composite thin film is shown in Fig. 3. The broad diffuse peak at around 25° is the signature of the amorphous nature and is appearing from the float glass substrate and the ceramic matrix, while other sharp peaks are due to the crystalline nature and appearing from Au crystallites, which have been assigned. The width of the crystalline peaks is the measure of the crystallites. If $\Delta\theta$ is the full width at half maximum of the diffraction peak at position 2θ, then the size of the crystallites can be estimated using Scherrer formula [25], $2R = C\lambda_0/(\Delta\theta \cos\theta)$. Neglecting Scherrer constant C, which is mainly depends on the shape of the crystallites and the (hkl) index of the diffraction peak, the

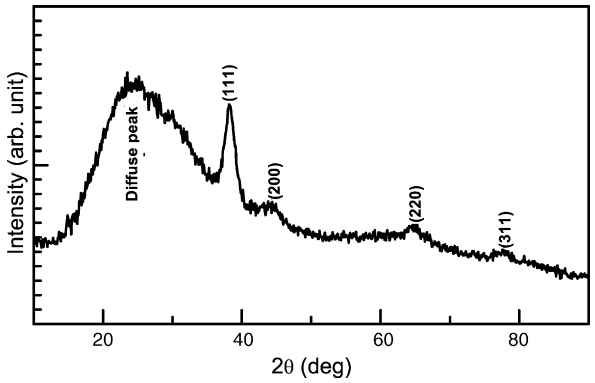

Fig. 3. Powder diffraction pattern of the Au/$LiNbO_3$ multilayer thin film. Broad diffuse peak is the signature of amorphous, while other sharp peaks have been assigned to Au-crystallites.

average size of the Au-crystallites is found to be $\sim$54 Å for the strong peak in Fig. 3, associated with (1 1 1) reflection. Powder diffraction pattern itself suggests the formation of small Au-nanocrystallites in $LiNbO_3$ amorphous matrix.

Optical absorption spectrum of the film is shown in Fig. 4. A broad absorption peak observed in the spectrum is due to the presence of Au nanoparticles in the film. The position (λ_p) of the peak at around 620 nm is quite high when compared with normal surface plasmon resonance of Au-nanoparticles. However, such deviation has been observed before [26] and can be well accounted for the large volume fraction of Au in the film. Considering the contribution of the volume fraction of metal nanoparticles, the modified Doyle's expression becomes [27,28]:

$$\lambda_p = \frac{2\pi c}{\omega_D}\left(1 + \frac{2+f}{1-f}\varepsilon_m\right)^{1/2}$$

where c is the velocity of light, ω_D is the Drude plasma frequency, f is the volume fraction of the metal particles, ε_m is dielectric constant of the medium. The size of the particle can be estimated using the relation, $R = v_F/\Delta\omega_{1/2}$, where, v_F is Fermi velocity and $\Delta\omega_{1/2}$ is the full-width at half-maximum of the absorption peak [29]. The above expressions help us to estimate R and f using other parameters from the literature [29]. The value obtained for $2R$ and f from the absorption spectrum are 31 Å and 0.19, respectively, which agrees well with those obtained from X-ray reflectivity and GISAXS analysis.

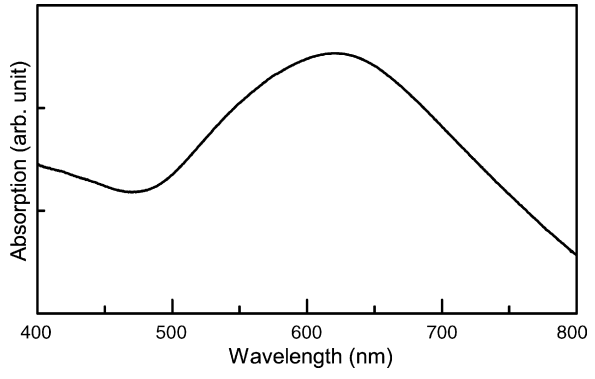

Fig. 4. Optical absorption spectrum of the Au/$LiNbO_3$ multilayer thin film.

4. Conclusion

The complete structure and morphology of a composite thin film, namely Au–$LiNbO_3$, where strong scatterers in large amount are present, have been successfully probed through laboratory source X-ray scattering measurements, which were mostly been carried out using synchrotron radiation facilities. It has been observed that Au-nanoparticles of size ∼3.2 nm are distributed in amorphous $LiNbO_3$ matrix in large volume fraction (∼0.23) having average interparticle separation ∼5.6 nm but no long-range periodicity other than z-direction. Optical properties agree well with the size and volume fraction of metal nanocrystallites in dielectric medium derived from X-ray scattering measurements.

Acknowledgement

The sample used here was provided by Prof. A. Gibaud and Prof. C. Sella, which is thankfully acknowledged.

References

[1] B.E. Warren, X-ray Diffraction Reading, Addison-Wesley, MA, 1969.
[2] I.K. Robinson, D.J. Tweet, Rep. Prog. Phys. 55 (1992) 599.
[3] T.P. Russell, Mater. Sci. Rep. 5 (1991) 171.
[4] V. Holy, U. Pietsch, T. Baumbach, High Resolution X-ray Scattering from Thin Films and Multilayers, Springer Tracts in Modern Physics, vol. 149, Springer, Berlin, 1999.
[5] J. Daillant, A. Gibaud (Eds.), X-ray and Neutron Reflectivity: Principles and Applications, Springer, Paris, 1999.
[6] M.K. Sanyal, A. Datta, S. Hazra, Pure Appl. Chem. 74 (2002) 1553.
[7] S.K. Sinha, E.B. Sirota, S. Garoff, H.B. Stanley, Phys. Rev. B 38 (1988) 2297.
[8] G.A. Niklasson, C.G. Granqvist, J. Appl. Phys. 55 (1984) 3382.
[9] C. Flytzanis, F. Hache, M.C. Kelin, D. Ricard, Ph. Roussignol, Prog. Opt. XXIX (1991) 323.
[10] A.P. Alivisatos, Science 271 (1996) 933.
[11] J. Schi, S. Gider, D.D. Awschalom, Science 271 (1996) 937.
[12] S. Link, M.A. El-Sayed, J. Phys. Chem. B 103 (1999) 8410.
[13] B.A. Korgel, D. Fitzmaurice, Phys. Rev. B 59 (1999) 14191.
[14] A. Naudon, D. Babonneau, Z. Metallkd. 88 (1997) 596.
[15] S. Hazra, A. Gibaud, A. Désert, C. Sella, A. Naudon, Physica B 283 (2000) 97.
[16] A. Gibaud, A. Baptiste, D.A. Doshi, C.J. Brinker, L. Yang, B. Ocko, Europhys. Lett. 63 (2003) 833.
[17] C. Revenant, F. Leroy, R. Lazzari, G. Renaud, C.R. Henry, Phys Rev. B 69 (2004) 035411.
[18] S. Hazra, A. Gibaud, C. Sella, Appl. Phys. Lett. 85 (2004) 395.
[19] (a) J.R. Levine, J.B. Cohen, Y.W. Chung, P. Georgopoulos, J. Appl. Cryst. 22 (1989) 528;
(b) J.R. Levine, J.B. Cohen, Y.W. Chung, Surf. Sci. 248 (1991) 215.
[20] L.G. Parratt, Phys. Rev. 95 (1954) 359.
[21] S. Kundu, S. Hazra, S. Banerjee, M.K. Sanyal, S.K. Mandal, S. Chaudhuri, A.K. Pal, J. Phys. D 31 (1998) L73.
[22] M. Rauscher, T. Salditt, H. Spohn, Phys. Rev. B 52 (1995) 16855.
[23] B.K. Vainshtein, Diffraction of X-rays by Chain Molecules, Elsevier, Amsterdam, 1966.
[24] A. Guinier, G. Fournet, Small-Angle Scattering of X-Ray, Wiley, New York, 1955.
[25] J.I. Langford, A.J.C. Wilson, J. Appl. Cryst. 11 (1978) 102.
[26] D.Y. Shang, H. Matsuno, Y. Saito, S. Suganomata, J. Appl. Phys. 80 (1996) 406.
[27] W.T. Doyle, Phys. Rev. 111 (1958) 1067.
[28] R.H. Doremus, J. Appl. Phys. 37 (1966) 2775.
[29] G.W. Arnold, J. Appl. Phys. 46 (1975) 4466.